The Effect of Iron Nano-inclusions in Multilayered Integrated Optical Waveguides

Isabelle G. de Moraes[1], **Anderson O. Silva**[1],
Maria Aparecida G. Martinez[1], **and Maria Thereza M. R. Giraldi**[2]

[1]Photonics Laboratory, Centro Federal de Educação Tecnológica Celso Suckow da Fonseca, Brazil
[2]Photonics Laboratory, Instituto Militar de Engenharia — IME, Brazil

Abstract— Nonorthogonal coupled mode theory is used to analyze the impact of iron nano-inclusion in the TE mode coupling between two integrated optical waveguides structures. In the first case, the nano-inclusion fractions are included in an identical manner in both waveguides, and in the second the nano-inclusion are added only in one of the waveguides. The structures beating lengths strongly depends on the inclusion filling factor and the thickness of the cladding layer. They reduce with increasing inclusion-filling factors, reaching a 70% and a 56% reduction with respect to the lossless case, for the identical and non-identical cases, respectively. Cladding thickness increases the beating length reducing the structure total power as filling factor increases, for the identical case, and depicting a inflection point for the non-identical case where the total power increases.

1. INTRODUCTION

In the last years, research on new materials and technologies together with established coupled mode theory, and electromagnetic numerical methods have featured the construction of novel integrated optical devices, like, directional couplers, power dividers, polarizers and isolators [1]. Most of these passive devices are based on the control of modal field, polarization, and others. In this work, we investigate the impact of iron nano-inclusions in the coupling of multilayered optical waveguides structure based on alternating InGaAsP and InP layers, operating at 1550 nm. The complex refractive index of the mixture (the host and inclusion materials) is obtained from iron experimental optical properties data and Maxwell-Garnett models [2]. The motivation is to use nano-inclusions to improve the coupler efficiency decreasing the beating length through the impact of the losses in the exchange power curve that is caused by the complex refractive index. The inclusions add losses to the system, creating a trade-off between decreasing beating length and output power. The behavior of the electrical field properties of the TE fundamental mode within the multilayer structure is analyzed by the use of the nonorthogonal Coupled Mode Theory [3, 4] for identical and non-identical cases. This theory enables to monitor the beating length and the power transfer along the waveguide propagation direction.

2. THEORETICAL FORMULATION

The multilayered structure of interest is shown in Figure 1. It consists of a five layers structure. Table 1 relates the layer number, material, complex refractive index, and thickness. The structure is based on the optical isolator proposed in [5, 6].

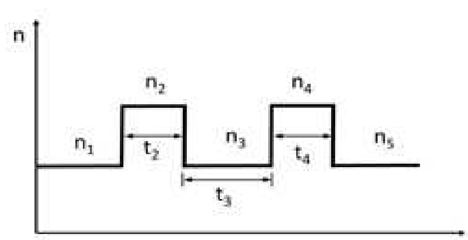

Figure 1: Multilayered waveguide structure.

The complex refractive index of the mixture is calculated considering InGaAsP host medium for filling factors of Fe inclusions ranging from 0.01% up to 0.2% at 1550 nm, X_i and Y_i for $i = 2, 4$, in Table 1, are the real and imaginary values of the complex refractive index values, estimated by the

Table 1: Structure parameters.

Layer	**Material**	n'	n''	**Thickness**
I	InP	3.162	0	Infinite
II	Fe-InGaAsP	X_2	Y_2	0.5
III	InP	3.162	0	t_3
IV	Fe-InGaAsP	X_4	Y_4	0.5
V	InP	3.162	0	Infinite

use of the Maxwell-Garnett formula. The Maxwell-Garnett mixing rule predicts the macroscopic permittivity (ϵ_{mix}) of a medium where iron particles are included in the InGaAsP host [7]:

$$\epsilon_{mix} = \epsilon_e + 3f\epsilon_e \frac{\epsilon_i - \epsilon_e}{\epsilon_i - 2\epsilon_e - f(\epsilon_i - \epsilon_e)} \tag{1}$$

In Equation (1), ϵ_e is the host material permittivity, ϵ_i is the Fe experimental permittivity at 1550 nm [8] and f is the volume fraction occupied by the inclusions. Table 2 lists the respective complex refractive indexes for each filling factor used in this investigation. The effective index is assumed as $n_{mix} = \sqrt{\epsilon_{mix}}$.

Table 2: Real and imaginary parts of the complex refractive index of the mixture.

f	**Re** (n_{mix})	**Im** (n_{mix})
0	3.3700	**0**
0.0001	3.3705	$4.1215\ 10^{-4}$
0.0005	3.3723	$2.0611\ 10^{-3}$
0.0010	3.3746	$4.1232\ 10^{-3}$
0.0015	3.3769	$6.1830\ 10^{-3}$
0.0020	3.3792	$8.2502\ 10^{-3}$

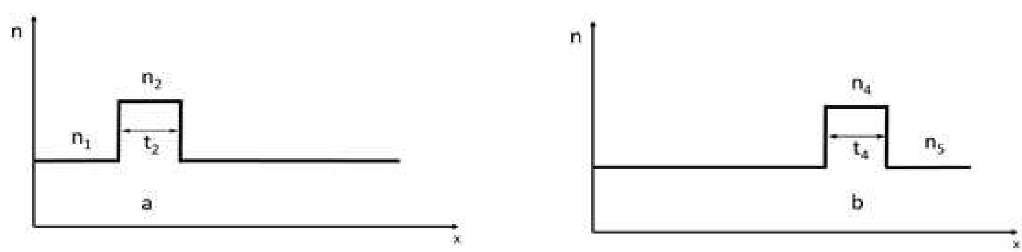

Figure 2: Waveguides a and b.

The coupled mode theory is a well-known approach to study waveguide coupling and its derivation can be found in the literature [3, 4]. The time convention adopted in this paper is $\exp(-i\omega t)$. Separating the structure in medium **a** and medium **b**, as depicted in Figure 2 and defining the fields and electrical permittivity distribution in each medium as $(E^{(a)}, H^{(a)})$, $\epsilon^{(a)}(x, y)$, $(E^{(b)}, H^{(b)})$ and $\epsilon^{(b)}(x, y)$ it is possible to express the electric field amplitude along propagation axis in waveguides **a** and **b**, $a(z)$ and $b(z)$ respectively, as a system of coupled differential equations whose matrix form is:

$$\frac{d}{dz}\left[\begin{array}{c} a(z) \\ b(z) \end{array}\right] = iC^{-1}S\left[\begin{array}{c} a(z) \\ b(z) \end{array}\right]. \tag{2}$$

C and S are 2×2 matrices, whose elements are defined as:

$$C_{pq} = \frac{1}{2} \iint E_t^{(q)} \times H_t^{(p)} \cdot \hat{z} dxdy \quad p, q = a \text{ or } b \tag{3}$$

$$S_{pq} = K_{pq} + \beta_p \left(\frac{C_{pq} + C_{qp}}{2} \right) \quad p, q = a \text{ or } b \tag{4}$$

$$K_{pq} = \frac{\omega}{4} \iint \Delta\epsilon^{(q)} \left(E_t^{(p)} \cdot E_t^{(q)} - \frac{\epsilon^{(q)}}{\epsilon} E_z^{(p)} E_z^{(q)} \right) \quad p, q = a \text{ or } b \tag{5}$$

$C_{aa} = C_{bb} = 1$ and C_{ab} and C_{ba} represent the crosspower coefficient, in other words, the result from an overlap integral between the evanescent fields in the cladding. In conventional theory [9] crosspower is null, because the transversal fields $E_t^{(q)}$ and $H_t^{(p)}$ are orthogonal. β_q express the propagation constant of each individual waveguide, obtained by Modal Analysis [10]. K_{pq} is the coupling coefficient, the integral between the transversal and longitudinal $(E_z^{(p)} E_z^{(q)})$ electrical fields of the individual waveguides, ω is the angular frequency, and the factor $\Delta\epsilon^{(q)} = \epsilon^{(q)} - \varepsilon$, express the perturbation effect that causes the coupling, where $\epsilon^{(q)}$ is the medium permittivity and ϵ is the background permittivity.

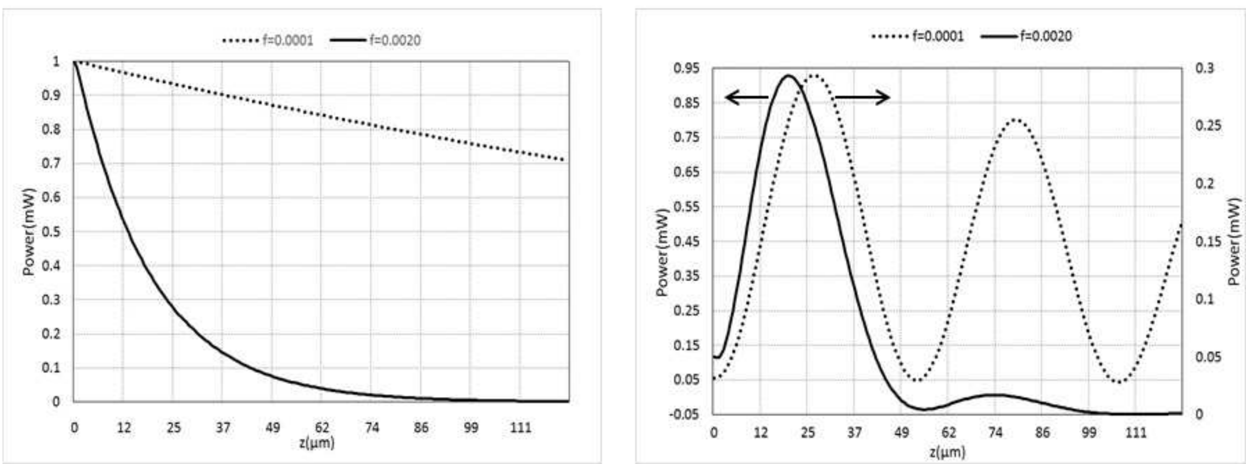

Figure 3: (a) Total power along z direction for $f = 0.0001$ (dotted line) and $f = 0.0020$ (solid line). (b) Power transferred along z direction for $f = 0.0001$ (dotted line) and $f = 0.002$ (solid line).

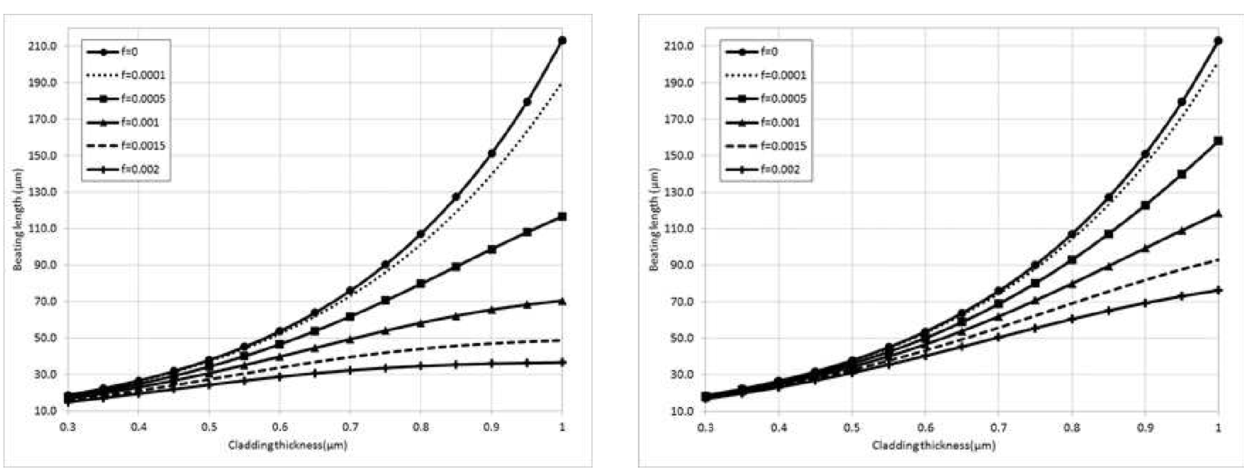

Figure 4: Beating length as a function of the cladding thickness for different inclusion filling factors. (a) $n_2 = n_4$ (identical case), (b) $n_4 = 3.37$ (non-identical case).

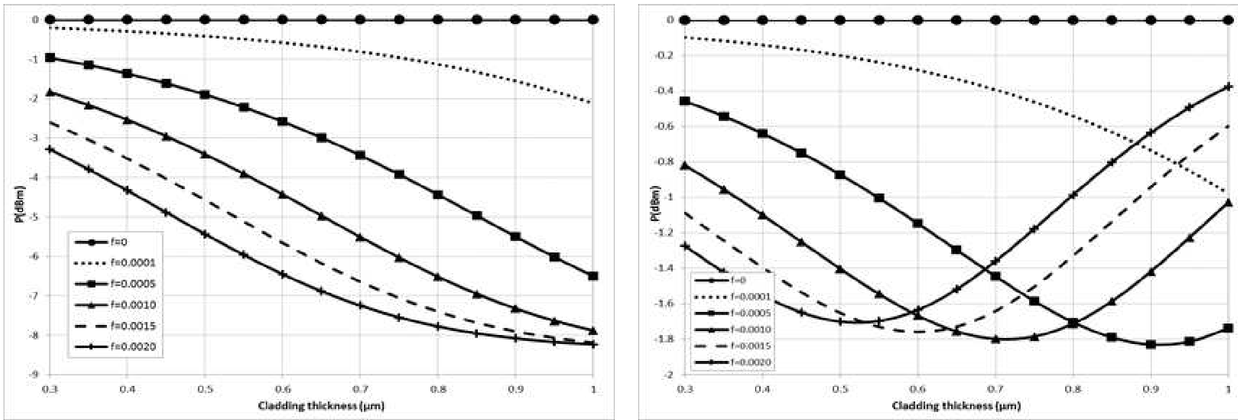

Figure 5: Total power (dBm) as a function of the cladding thickness for different values of inclusion fraction (a) $n_2 = n_4$ (identical case), (b) $n_4 = 3.37$ (non-identical case).

3. NUMERICAL RESULTS

The impact of Fe filling factor is analyzed through the solution of Equation (2), considering $a(0) = 0$ and $b(0) = 1$, for identical waveguides ($n_2 = n_4$) and for non-identical waveguides ($n_4 = 3.37$). The total power in the structure and the power transferred to waveguide **a**, in the identical waveguide case, for $f = 0.0001$ and $f = 0.002$, are shown in Figure 3(a) and Figure 3(b), respectively. In Figure 3(a), the power decay along the structure is faster for higher inclusion factor. An increase in inclusion filling factor decreases the structure beating length, which is depicted in Figure 3(b), by the relative displacement between the curves. The inclusion adds a relative shift in power exchange oscillation between the waveguides, like a resistive element does in a RCL circuit. The structures beating length as a function of cladding thickness for different filling factors values are shown in Figures 4(a) and 4(b), for the identical and non-identical cases, respectively. An increase in cladding thickness increases the structure beating length due to a weaker coupling between the waveguides. Further, the impact of nano-inclusion filling factors in beating lengths is evident for cladding thickness greater than 0.6 µm. For $f = 0.002$ and cladding thickness of 0.8 µm, the beating length reduces in 70% compared to the lossless situation ($f = 0$) for the identical case, while it reduces 56% for the non-identical case. The structure output power after one beating length as a function of cladding thickness is shown, for different values of nano-inclusion factors, in Figures 5(a) and 5(b) for the identical and non-identical cases, respectively. For the identical case, and cladding layer thickness up to 1 µm, the structure output power decreases with inclusion filling factor as shown in Figure 5(a). The structure reaches up to 8 dB loss for $f = 0.002$ when compared to the lossless situation ($f = 0$). For the non-identical case, the total power behavior changes considerably. The output power decreases up to a certain cladding thickness value and then starts to increase, reducing the structure losses. This inflection point marks the filling factor for which the beating length reduction due to the added losses overcomes its increase for a certain cladding thickness.

4. CONCLUSIONS

We used the non-orthogonal coupled mode theory to analyze the impact of iron nano-inclusions in multilayer integrated optical structures (identical and non-identical). The structures beating length and total power depend on the inclusion filling factor and the cladding thickness. Overall, the inclusion filling factor decreases the structure beating length while the cladding thickness increases it. Nonetheless, the total power in the structures behaves quite differently for both cases. In the identical case, the structure total power decreases with cladding and with inclusion filling factor. For the non-identical case, as one of the waveguide is lossless, the total output power decreases with cladding thickness and filling factor until a certain cladding thickness and then increases. Part of the light propagates through the lossless waveguide, turning the impact of cladding thickness not as relevant as in the identical case. Finally, we demonstrate that suitably controlling the nano-inclusion filling factor and cladding thickness, particularly for the fundamental TE modes, a more efficient multilayer coupling structure, with reduced beating length and losses can be designed.

ACKNOWLEDGMENT

Isabelle G. de Moraes would like to thank the support from CEFET/RJ through the Program PIBIC. The authors acknowledge CAPES and CNPq for partially supporting this work.

REFERENCES

1. Dai, D., J. Bauters, and J. E. Bowers, "Passive technologies for future large-scale photonic integrated circuits on silicon: Polarization handling, light non-reciprocity and loss reduction," *Light: Science & Applications*, 1–12, 2012.
2. Sihvola, A., "Homogenization of a dielectric mixture with anisotropic spheres in anisotropic background," *Electromagnetics*, Vol. 17, No. 3, 269–286, 1997.
3. Chuang, S.-L., "A coupled mode formulation by reciprocity and a variational principle," *Journal of Lightwave Technology*, Vol. 5, 5–15, 1987.
4. Hardy, A. and W. Streifer, "Coupled mode theory of parallel waveguides," *Journal of Lightwave Tecnology*, Vol. 3, 1135–1146, 1985.
5. Shirato, Y., Y. Shoji, and T. Misumoto, "High isolation in silicon waveguide optical isolator employing nonreciprocal phase shift," *Proceedings of the Optical Fiber Communication Conference*, United States, 2013.
6. Hammer, J. M., G. A. Evans, G. Ozgur, and J. K. Butler, "Isolators, polarizers, and other optical waveguide devices using a resonant-layer effect," *Journal of Lightwave Technology*, Vol. 22, No. 7, 1754–1763, 2004.
7. Sihvola, A., "Homogenization of a dielectric mixture with anisotropic spheres in anisotropic background," *Electromagnetics*, Vol. 17, No. 3, 269–286, 1997.
8. Krinchik, G. S. and V. A. Artemjev, "Magneto-optic properties if nickel, iron, and cobalt," *Jounal of Applied Physics*, Vol. 39, No. 2, 1276–1278, 1968.
9. Yariv, A., "Coupled-mode theory for guided-wave optics," *IEEE Journal of Quantum Electronics*, Vol. 9, No. 9, 919–933, 1973.
10. Marcuse, D., *Theory of Optical Waveguides*, Academic Press, New York, 1974.